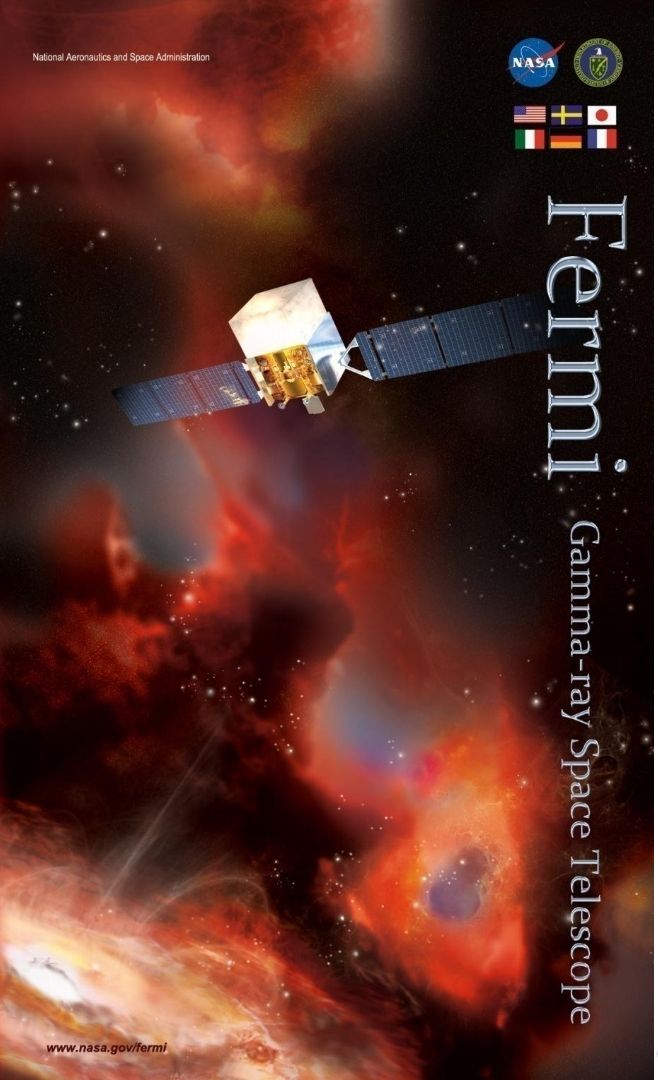

GeV flares characteristic in blazars

Janeth Valverde
UMBC / NASA GSFC

Motivation

Long-baseline, multi-wavelength (MWL), well-sampled, quasi-simultaneous data in the entire spectrum are needed:

- For time-domain and multi-messenger astrophysics discoveries, e.g. TXS 0506+056.
- To investigate active galactic nuclei (AGN) variability, e.g. structure, nature of particles in emission region, timescales of underlying processes and associated spectral changes.

Difficult to obtain observation over a long time, simultaneous, and in the entire spectrum.

In the γ-ray band, Fermi-LAT aperture photometry LCs are easily contaminated by nearby variable sources.

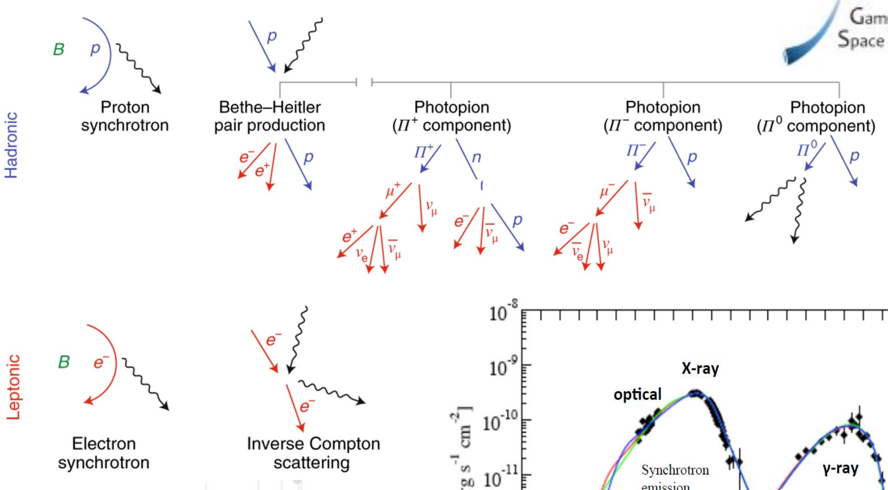

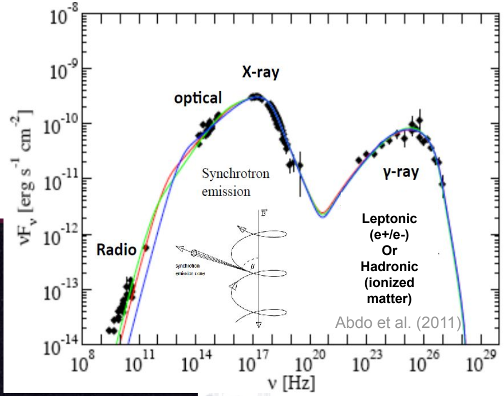

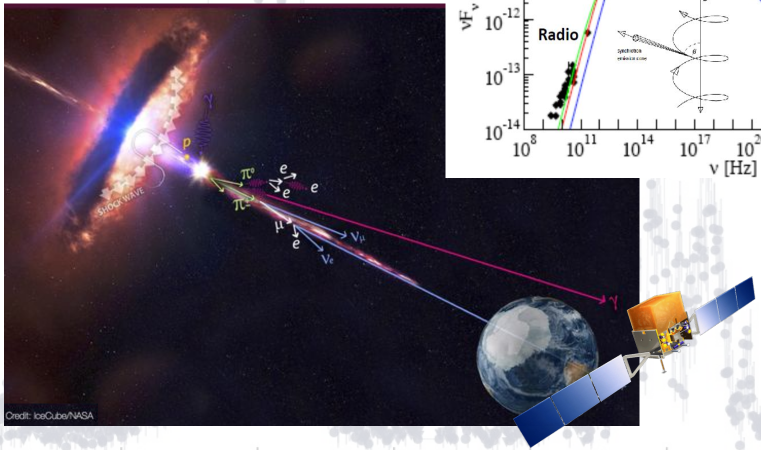

Blazar classification

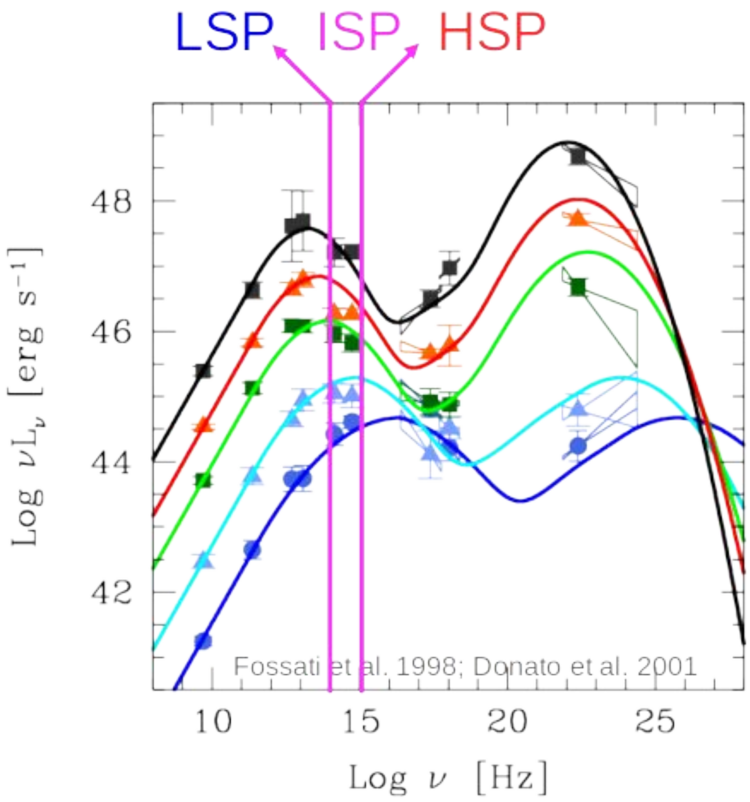

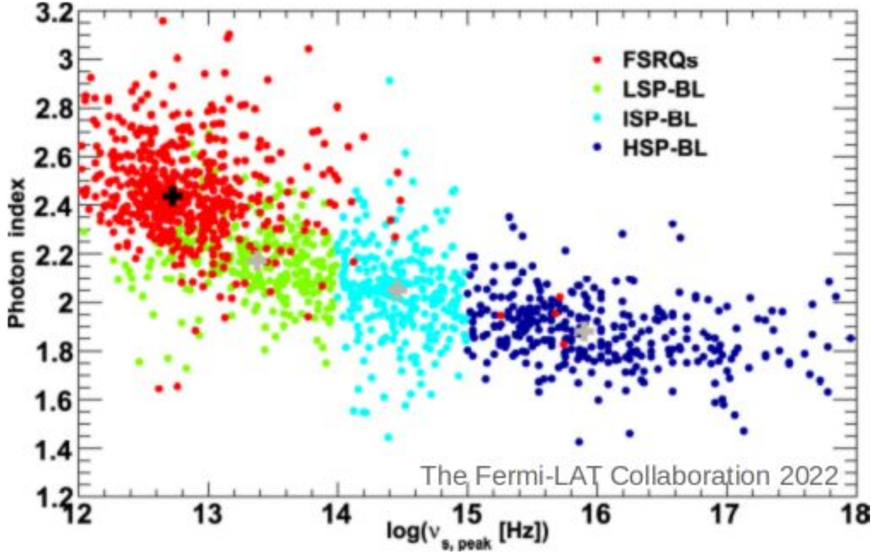

BL Lacs subtypes: Low-, intermediate- or high-synchrotron-peaked (LSP, ISP, HSP; Abdo et al. 2010). Based in Padovani & Giommi (1995; ratio 5 GHz/1 keV flux) for BL Lac objects: LBL, IBL, HBL.

Blazar classification

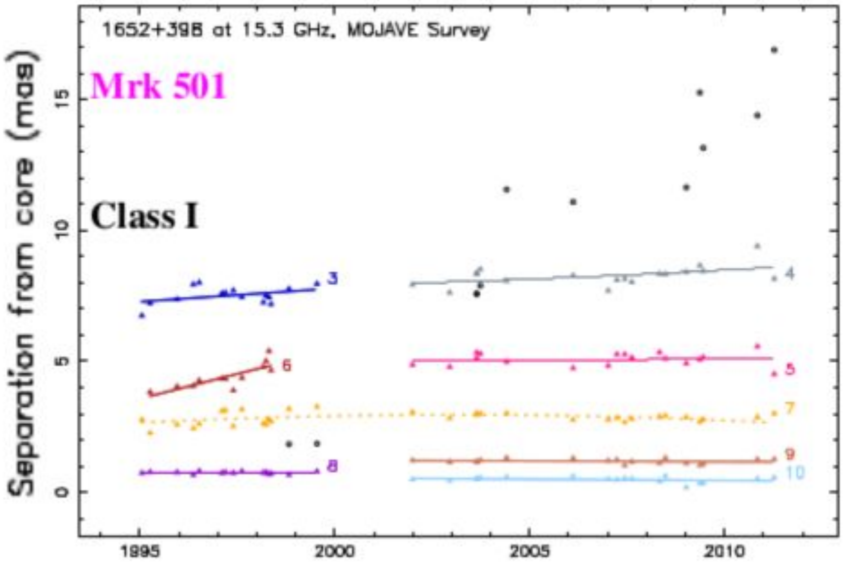

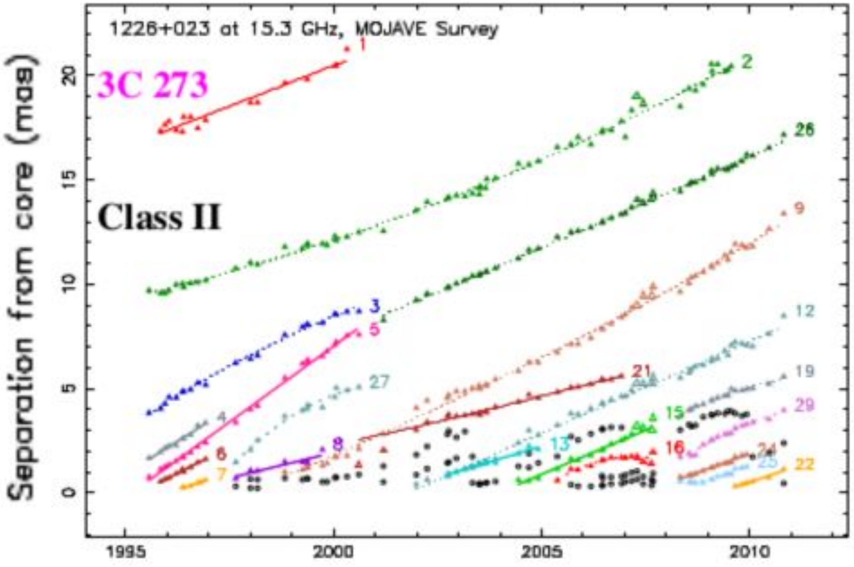

More recent classification based on the kinematics of jet radio components (Hervet et al. 2016):

- Class I: HBLs.
- Class II: FSRQs.
- Class I/II: IBLs, components close to the core in relative motion.

Blazar variability

- Variability timescales from years to minutes.
- Rapid variability challenge theoretical models:
    - Large δ ($\delta = \frac{1}{\gamma(1-\beta\cos(\theta))}, \quad \gamma = (1-\beta^2)^{-1/2}$)
    - Long cooling time in hadronic models
    - Can be produced by proton synch with very high energy protons & extremely large B.
- Possible quasi-periodic flux modulation.

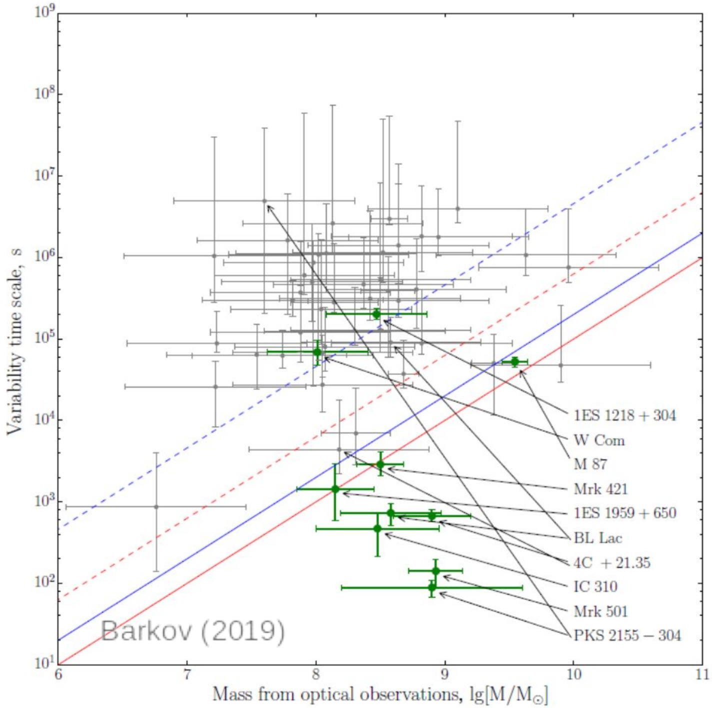

PG 1553+113: Period ~2yrs?

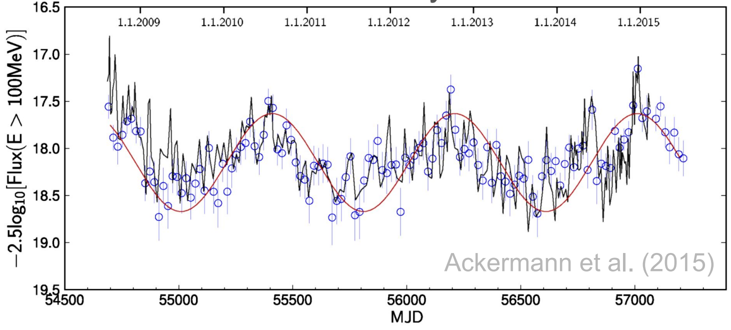

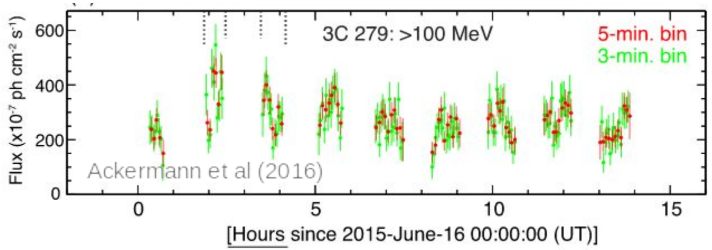

Fermi-LAT

ROI=Region of Interest 10^{o}

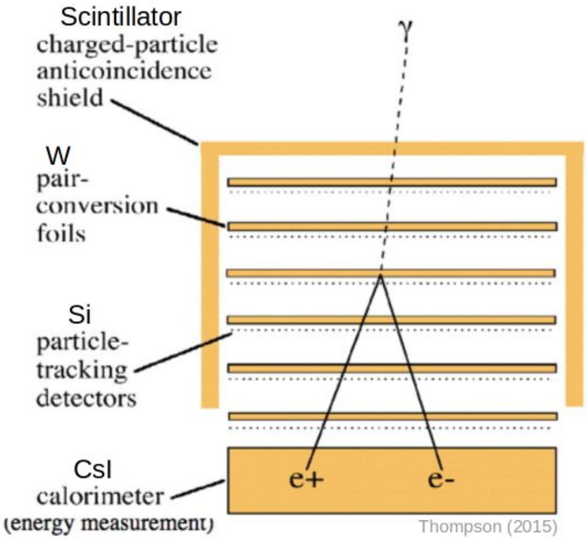

Thompson (2015)

Isotropic diffuse γ-ray emission.

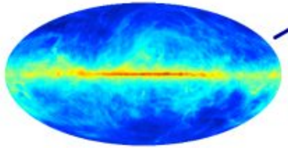

Galactic diffuse γ-ray emission.

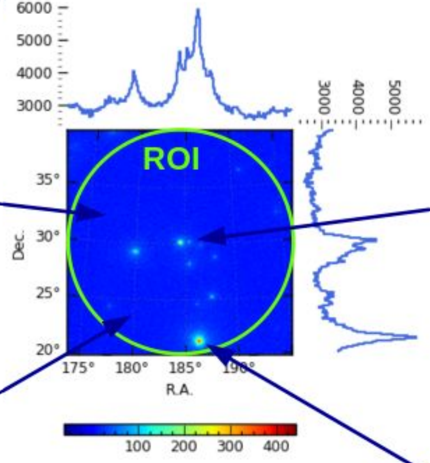

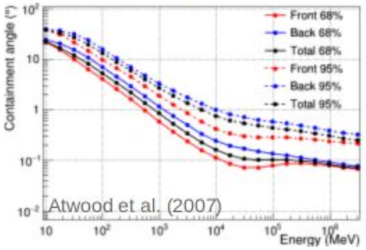

Atwood et al. (2007)

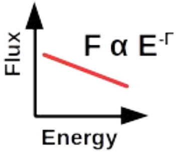

Power law

Emission from point-like sources.

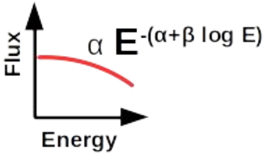

$\gamma \rightarrow e^{+} + e^{-}$

Light curve analysis

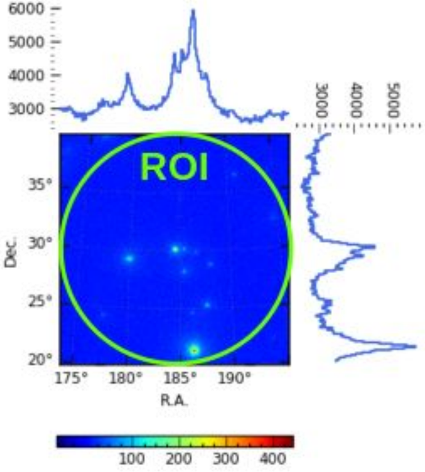

Cuts
Exposure
Cube maps
…
pre-calculations
Likelihood fit
Source maps
Sanity checks

Use fit model for SED/LC

Light curve: N time bins

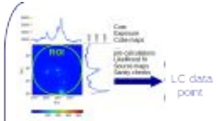
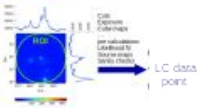

…
Thousands if source is bright enough.
…

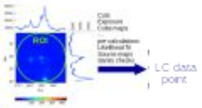

+ Sanity checks. Method validation. Run more refined LC if required by higher level analyses.

SED: M energy bins

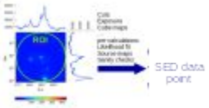

…
a few dozens.
…

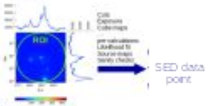

+ Sanity checks. Run SED for smaller time ranges as required by higher level analyses.

Multi-wavelength emission

[ApJ 891 (2020) 170](ApJ 891 (2020) 170)

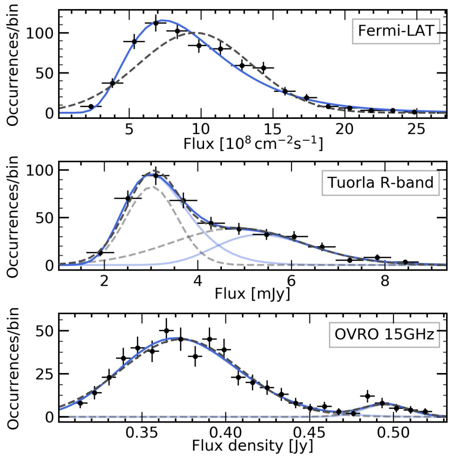

- TeV γ-rays
- GeV γ-rays
- X-ray
- UV-Optical
- Optical
- Optical polarization
- Radio

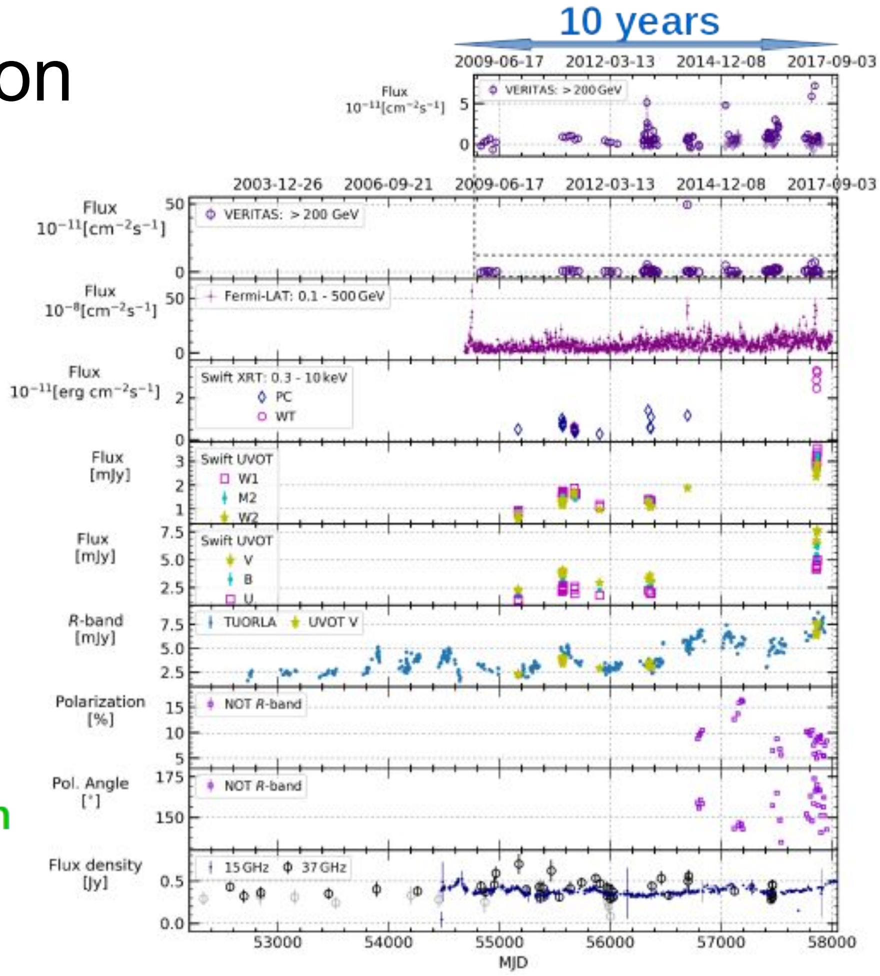

Trends & flux-flux correlations

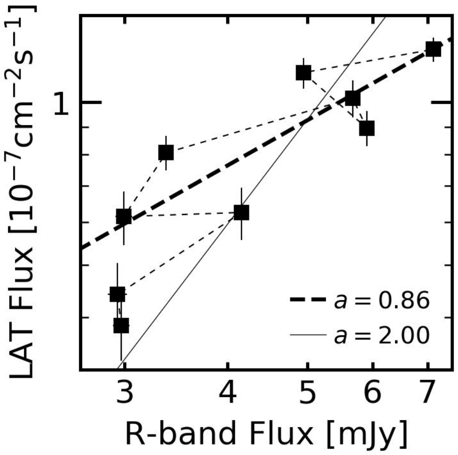

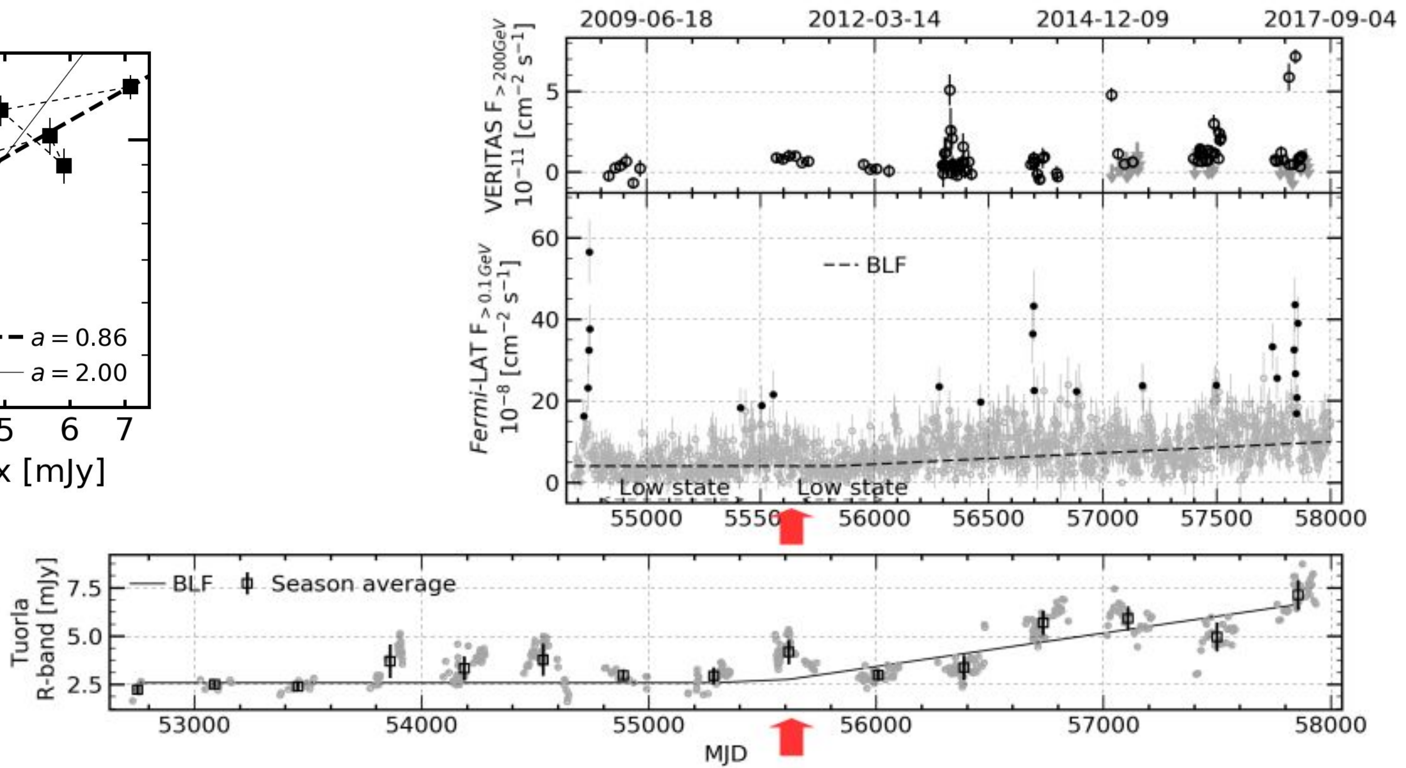

Broadband SED: Low vs flaring states

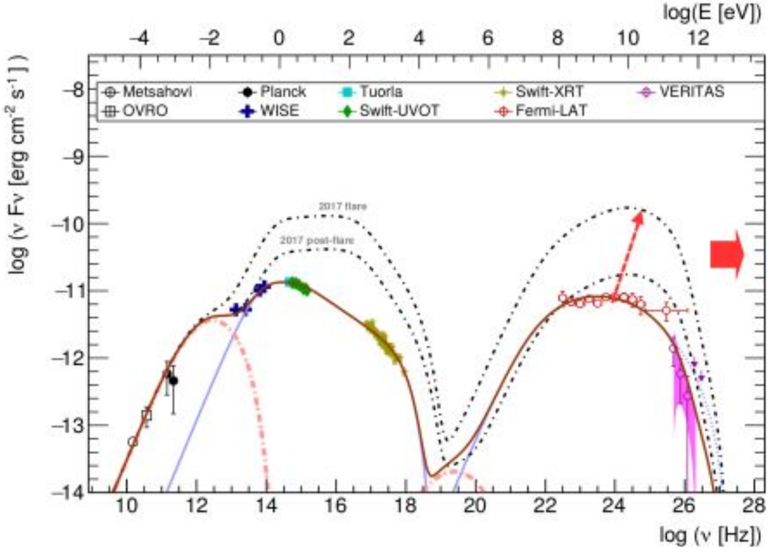

$K_1 \times 3$
$B \times 2.4$
$\gamma_{brk} \times 4.5$
$n_2 \times 1.2$

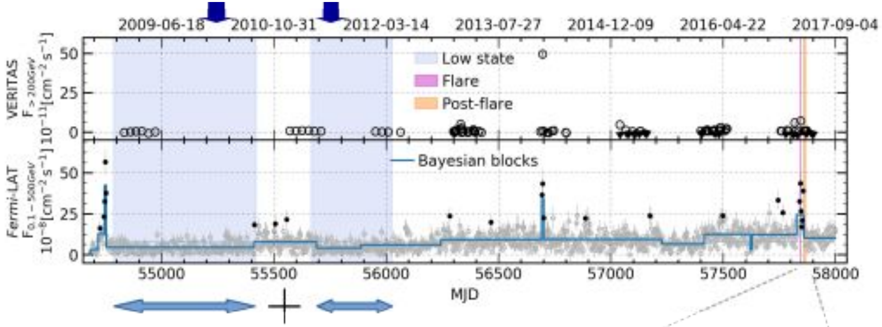

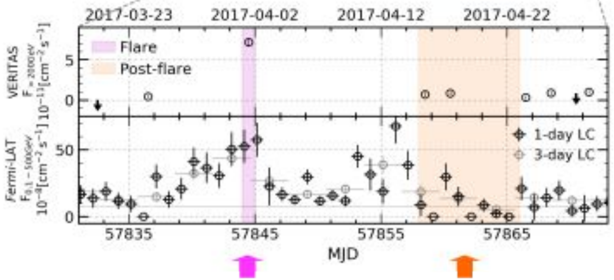

Flare Post-flare

Dramatic synchrotron peak shift

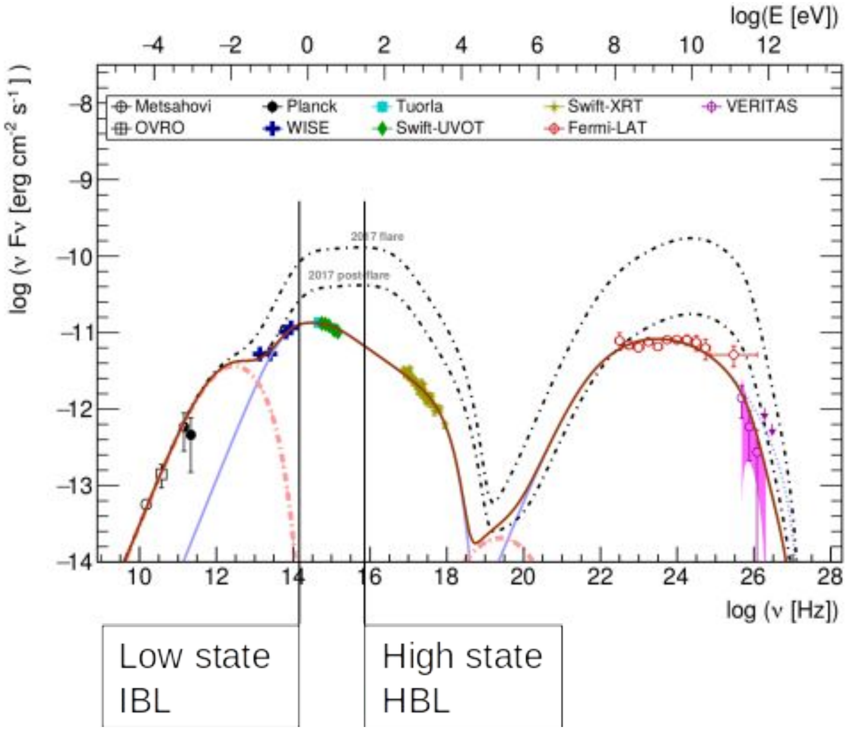

In 4LAC

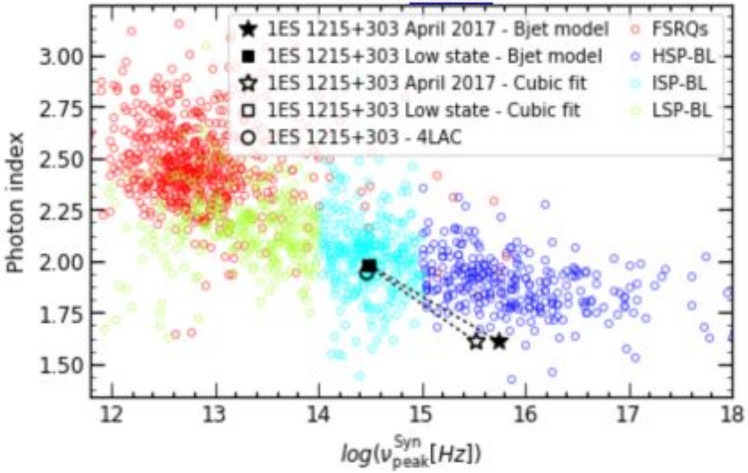

Largest IR-X-ray synch. peak shift in a BL Lac.

Possibly due to more efficient adiabatic/advective cooling during the flare state.

TeV FSRQs: PKS 1222+216 & Ton 599

[ApJ 924 (2022) 95]

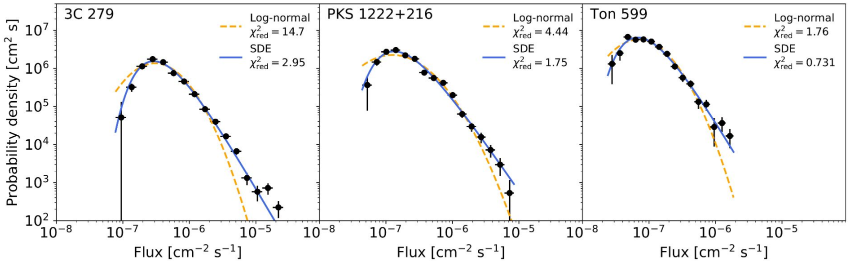

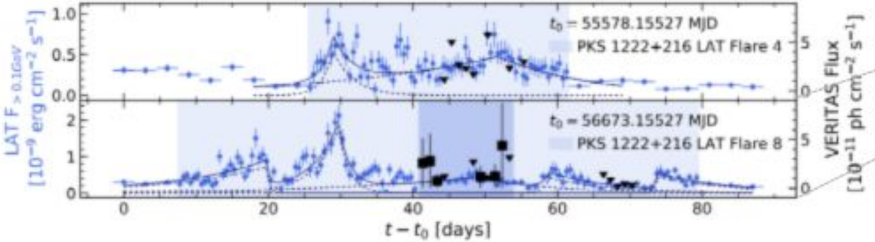

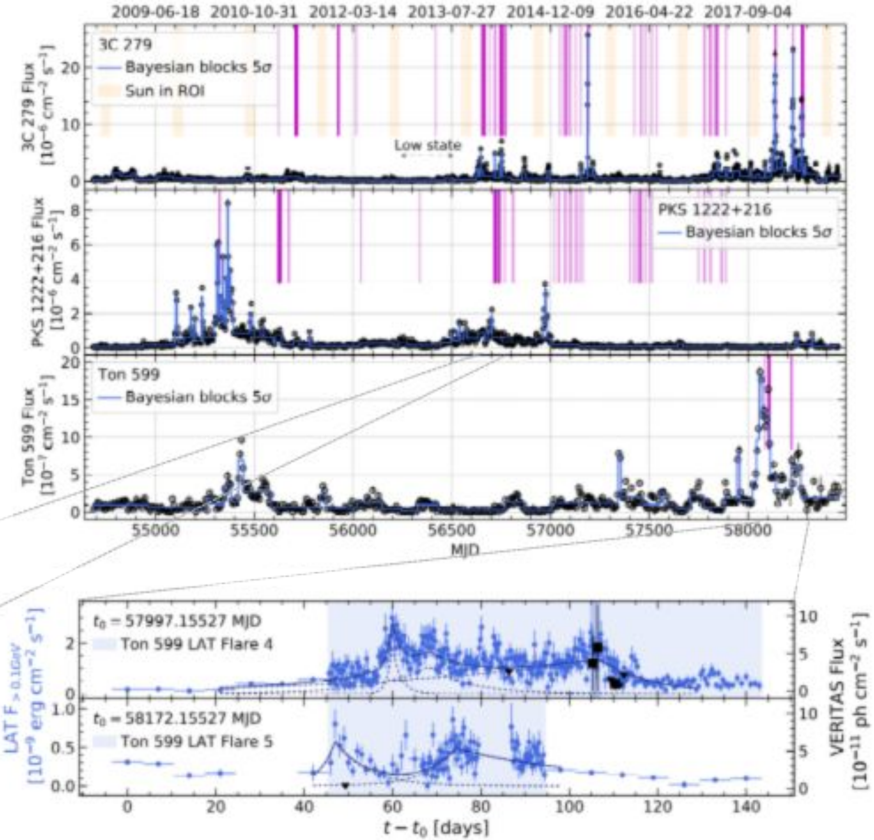

3C 279

Table 8. Results of the LAT flare profile fits for 3C 279.

Amplitude (F_0) (10^{-9} erg cm^{-2} s^{-1})	t_{peak} (MJD)	t_{rise} (min.)	t_{decay} (min.)	Constant ($F_{const.}$) (10^{-9} erg cm^{-2} s^{-1})
Flare 1 (MJD 56645.655 – 56647.655): χ^2/d.o.f.= 12.05/8 = 1.51				
9.56 ± 1.07	56646.330 ± 0.033	130 ± 45	674 ± 73	0.28 ± 0.06
Flare 2 (MJD 56717.655 – 56718.655): χ^2/d.o.f.= 16.63/10 = 1.66				
4.40 ± 0.70	56718.142 ± 0.043	445 ± 95	307 ± 86	0.55 ± 0.07
Flare 3 (MJD 56749.655 – 56754.655): χ^2/d.o.f.= 69.98/34 = 2.06				
7.27 ± 0.64	56750.382 ± 0.015	229 ± 25	267 ± 42	N.A.
2.78 ± 1.15	56751.238 ± 0.024	140 ± 82	69 ± 47	N.A.
4.80 ± 0.37	56752.532 ± 0.067	2001 ± 116	631 ± 136	N.A.
Flare 4 (MJD 57186.655 – 57190.655): χ^2/d.o.f.= 77.31/19 = 4.07				
12.07 ± 0.67	57187.446 ± 0.031	378 ± 46	1784 ± 147	N.A.
9.79 ± 2.29	57188.425 ± 0.028	216 ± 101	155 ± 64	N.A.
21.72 ± 1.59	57189.069 ± 0.008	137 ± 18	512 ± 55	N.A.
12.41 ± 1.30	57189.532 ± 0.010	220 ± 63	77 ± 25	N.A.
Flare 5 (MJD 58116.655 – 58119.655): χ^2/d.o.f.= 54.70/29 = 1.89				
3.72 ± 0.20	58118.171 ± 0.069	1278 ± 220	2521 ± 309	0.06 ± 0.11
Flare 6 (MJD 58130.655 – 58141.655): χ^2/d.o.f.= 141.28/72 = 1.96				
7.08 ± 1.01	58134.520 ± 0.055	3719 ± 390	421 ± 259	N.A.
10.95 ± 3.74	58135.229 ± 0.053	718 ± 232	3535 ± 1394	N.A.
11.78 ± 7.00	58136.266 ± 0.048	349 ± 160	1839 ± 1055	N.A.
3.44 ± 0.66	58139.546 ± 0.033	233 ± 175	6119 ± 1824	N.A.
Flare 7 (MJD 58168.655 – 58173.655): χ^2/d.o.f.= 78.81/58 = 1.36				
2.36 ± 0.50	58172.345 ± 0.242	8540 ± 4159	4458 ± 2319	0.45 ± 0.59
Flare 8 (MJD 58222.655 – 58230.655): χ^2/d.o.f.= 177.25/106 = 1.67				
5.29 ± 1.29	58224.773 ± 0.105	1996 ± 716	5899 ± 4035	N.A.
17.70 ± 2.01	58227.945 ± 0.004	**36 ± 13**	329 ± 131	N.A.
16.42 ± 1.87	58228.323 ± 0.012	140 ± 54	115 ± 48	N.A.
5.59 ± 1.69	58227.139 ± 0.133	3816 ± 1450	4077 ± 2080	N.A.
Flare 9 (MJD 58239.655 – 58247.655): χ^2/d.o.f.= 46.25/34 = 1.36				
2.96 ± 0.40	58241.258 ± 0.149	2546 ± 595	2226 ± 1088	N.A.
3.27 ± 0.25	58245.648 ± 0.133	3080 ± 1384	3028 ± 303	N.A.
Flare 10 (MJD 58268.655 – 58275.655): χ^2/d.o.f.= 75.80/55 = 1.37				
6.23 ± 9.46	58269.171 ± 0.182	73 ± 236	177 ± 102	N.A.
8.81 ± 0.84	58270.137 ± 0.107	2392 ± 243	2449 ± 956	N.A.
4.46 ± 1.91	58271.223 ± 0.088	477 ± 431	5824 ± 862	N.A.

NOTE—The smallest variability time found is indicated in boldface.

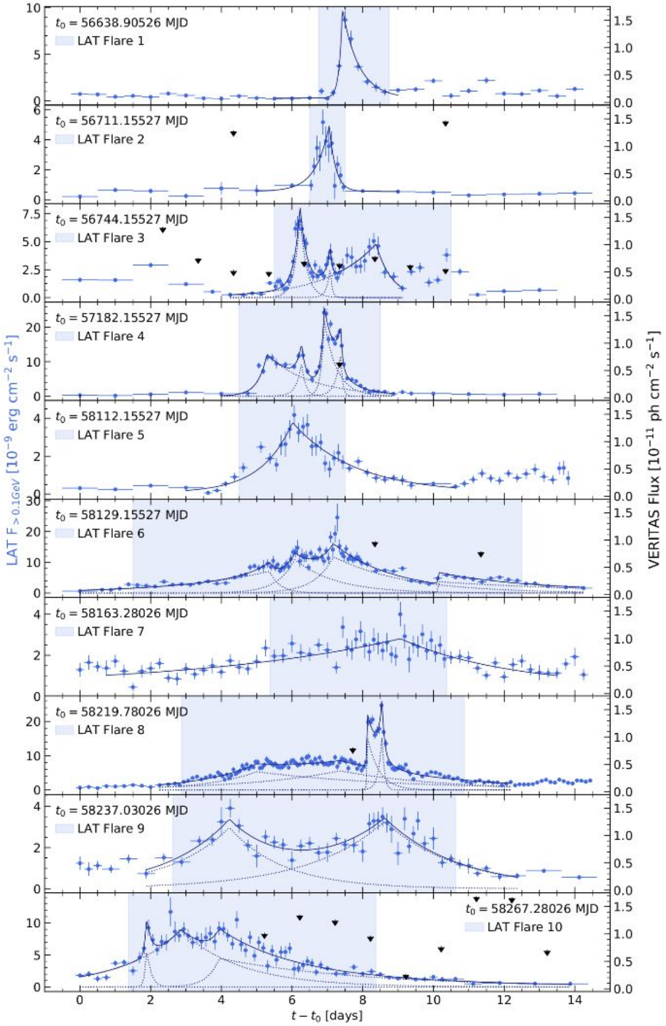

3C 279

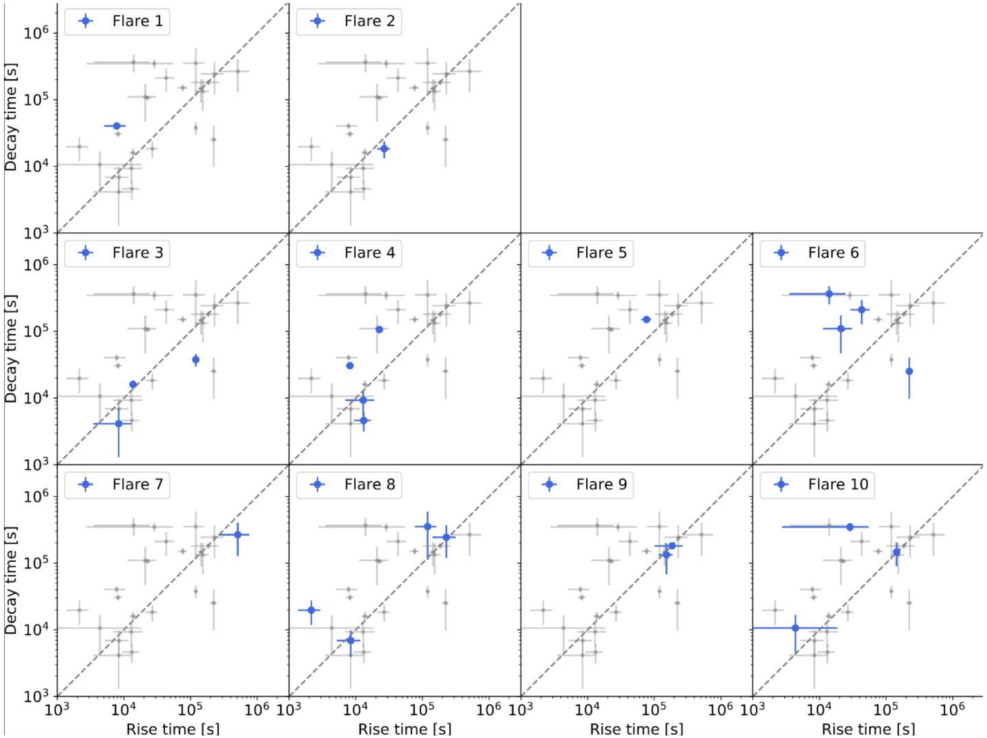

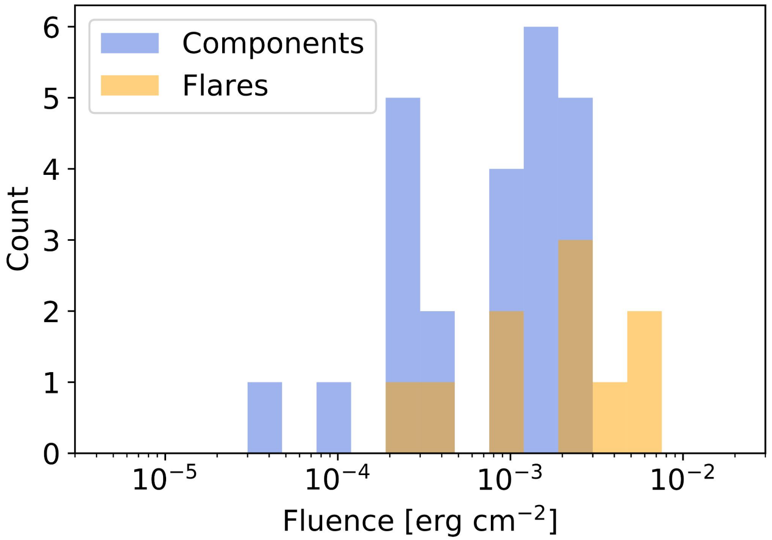

Fluence distributions of the individual flare components and flares resolved for 3C 279 during the first 11 years of the Fermi-LAT mission.

The Fermi Large Area Telescope
Light Curve Repository

https://fermi.gsfc.nasa.gov/ssc/data/access/lat/lcr/

ApJS (2023), 265, 31

Fermi Gamma-ray Space Telescope

Fermi-LAT LCs.

Public database since Dec 2021.

Publication ready.

1525 sources (26% of 4FGL-DR2).

3-, 7- & 30-day cadence.

Spectral information.

Entire mission (> 15 years).

Continuously updated.

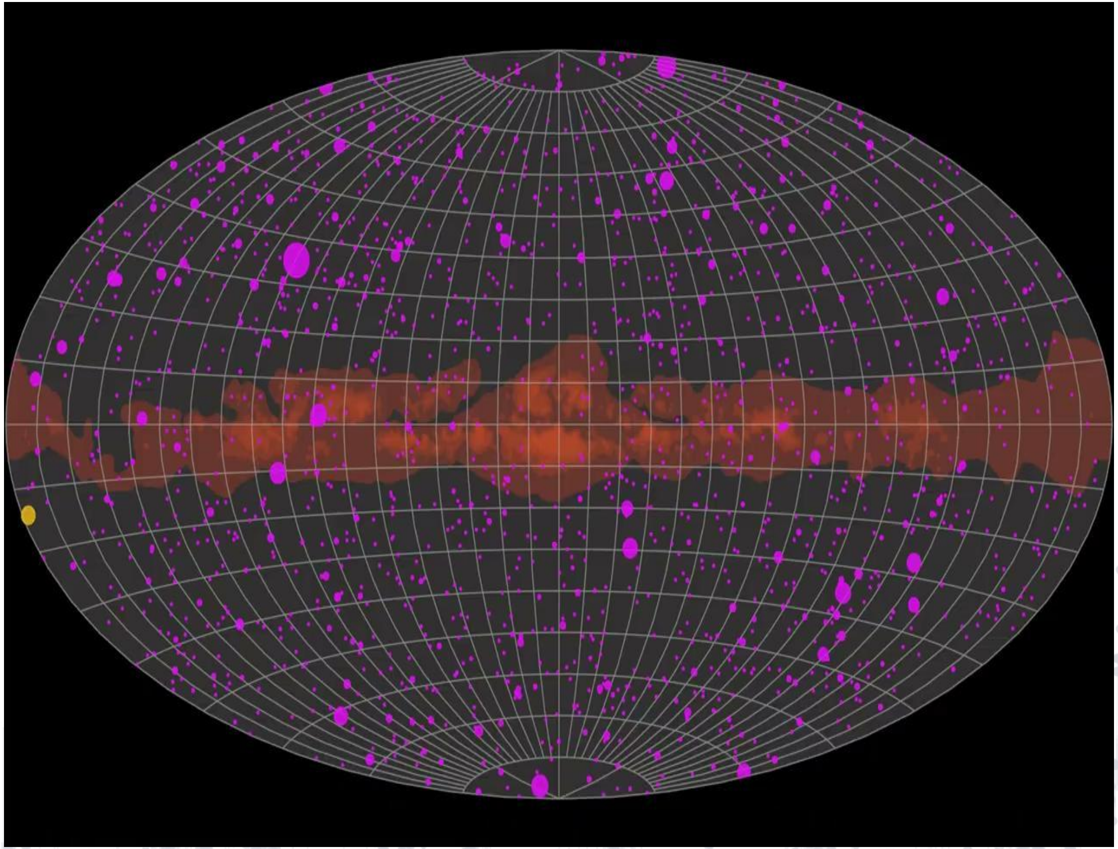

LCR computational strategy

A major challenge of producing likelihood light curves is the computational expense.

the LCR distributes the analyses of the light curve bins to separate nodes in a computer cluster hosted at the SLAC National Accelerator Laboratory.

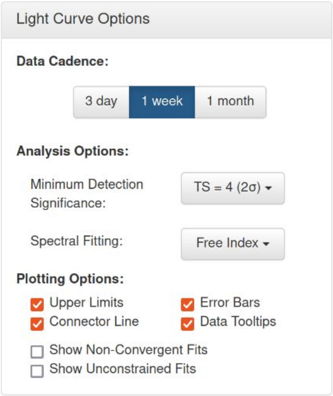

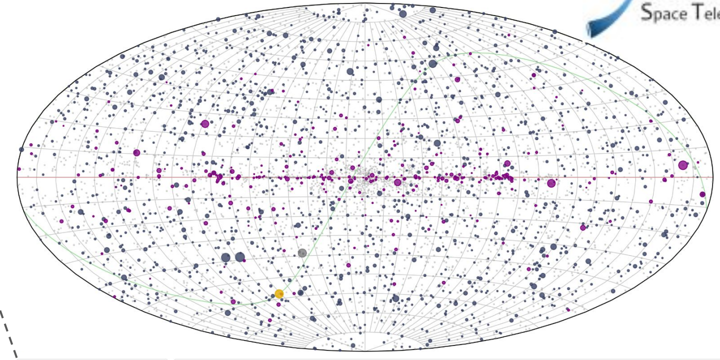

- Sources with variability index > 21.67 over 10 yearly points indicates <1% chance of being a steady source.
- Unbinned maximum likelihood, iterative, fit with decreasing tolerance [1, 1e-4, 1e-8].
- Only variable sources free in 12° ROI. Two-step fit strategy:
  - 1st fit: only normalization free & spectral index fixed to catalog value.
  - 2nd fit: normalization & a spectral index free; e.g. photon index for power-law or α for logparabola (β is fixed).
- Flux extracted when TS>1. 95% Bayesian ULs when TS<9.

LCR population

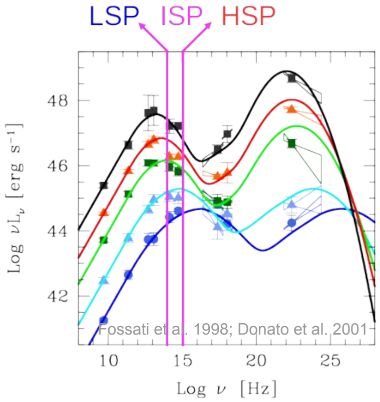

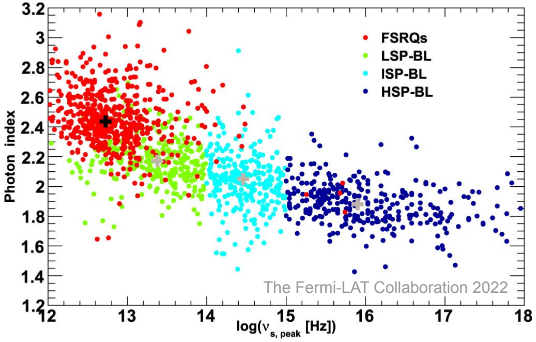

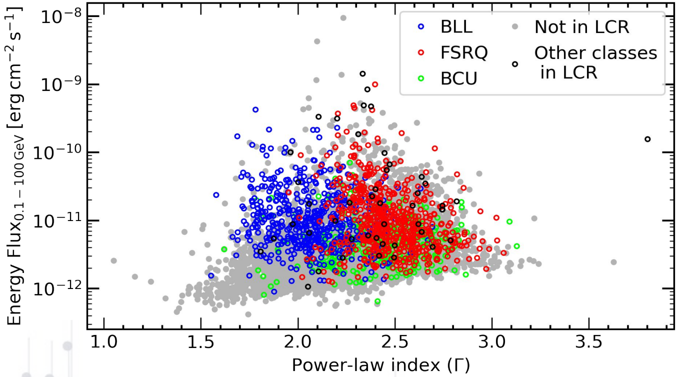

- 38% FSRQs, 31% BL Lac & 24% BCU of LCR sample, or 77%, 36% & 26% of their respective 4FGL-DR2 class.

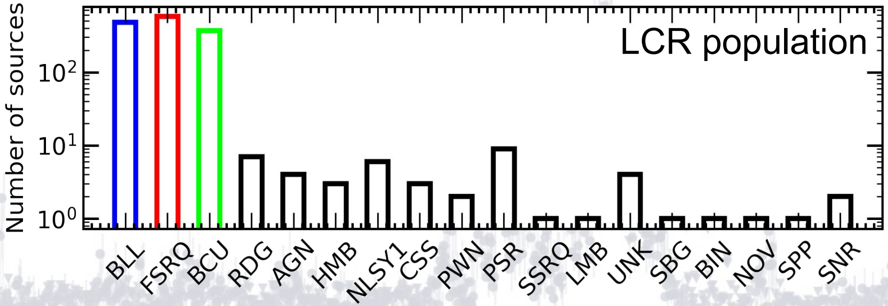

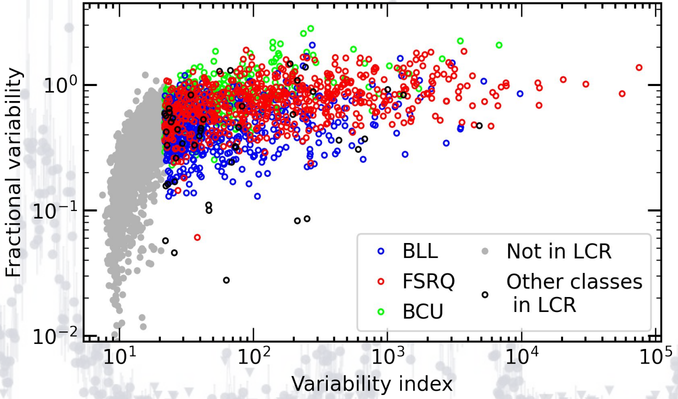

Website

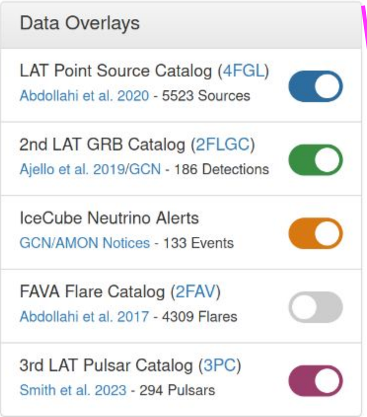

Source ID	RA	Dec	Gal l	Gal b	Association	Class	Variability Index	Photon Flux 1-100 GeV	Eenrgy Flux 1-100 GeV	Average Significance
4FGL J0000.3-7355	0.098	-73.922	307.709	-42.730			14.023	1.421e-10	1.622e-12	6.905
4FGL J0000.5+0743	0.138	7.727	101.656	-53.029			17.717	1.730e-10	2.272e-12	5.369
4FGL J0001.2+4741	0.313	47.686	114.250	-14.338	B3 2358+474	bcu	20.019	1.216e-10	1.407e-12	4.092
4FGL J0001.2-0747	0.315	-7.797	89.033	-67.305	PMN J0001-0746	bll	33.229	8.232e-10	9.171e-12	23.369
4FGL J0001.5+2113	0.382	21.218	107.649	-40.168	TXS 2358+209	fsrq	1564.418	1.359e-9	2.614e-11	44.135
4FGL J0001.6-4156	0.416	-41.943	334.226	-72.029	2MASS J00013275-4155252	bcu	16.149	3.049e-10	3.913e-12	15.611
4FGL J0002.1-6728	0.538	-67.475	310.085	-48.963	SUMSS J000215-672653	bcu	13.479	2.417e-10	2.888e-12	13.141

Link to main page

Analysis description & caveats

Download codes
Also pyLCR

Diagnostic plots

Two types of light curves:

- Index fixed
- Index free

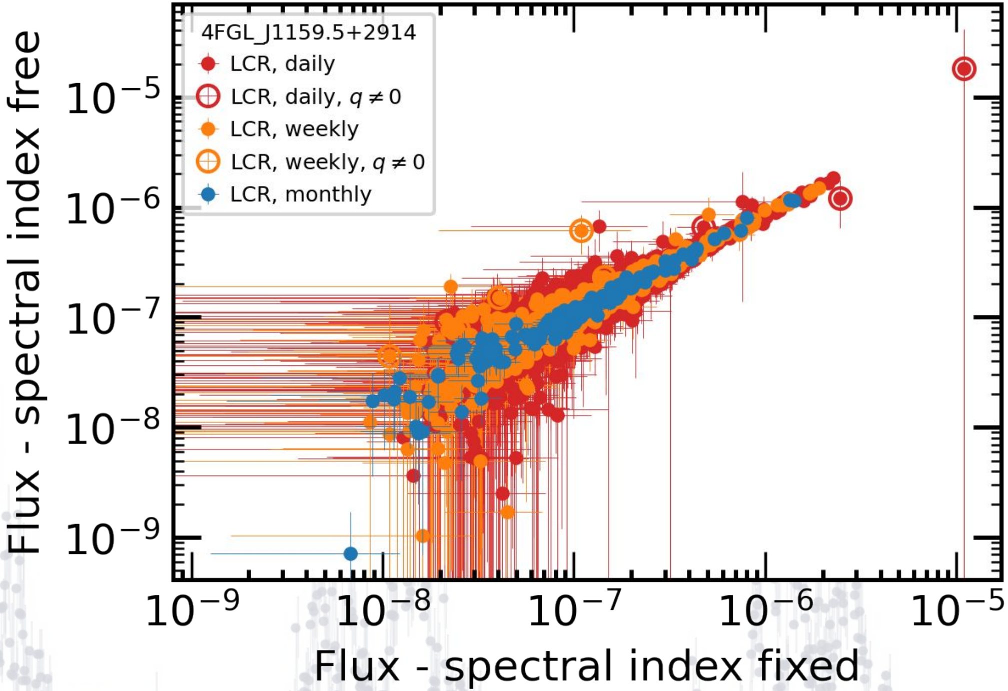

Ton 599: Comparison of the fluxes in time bins obtained with the fitting pipeline keeping the spectral index fixed vs letting the spectral index be free. Empty circles indicate results from analyses that did not converge.

Diagnostic plots

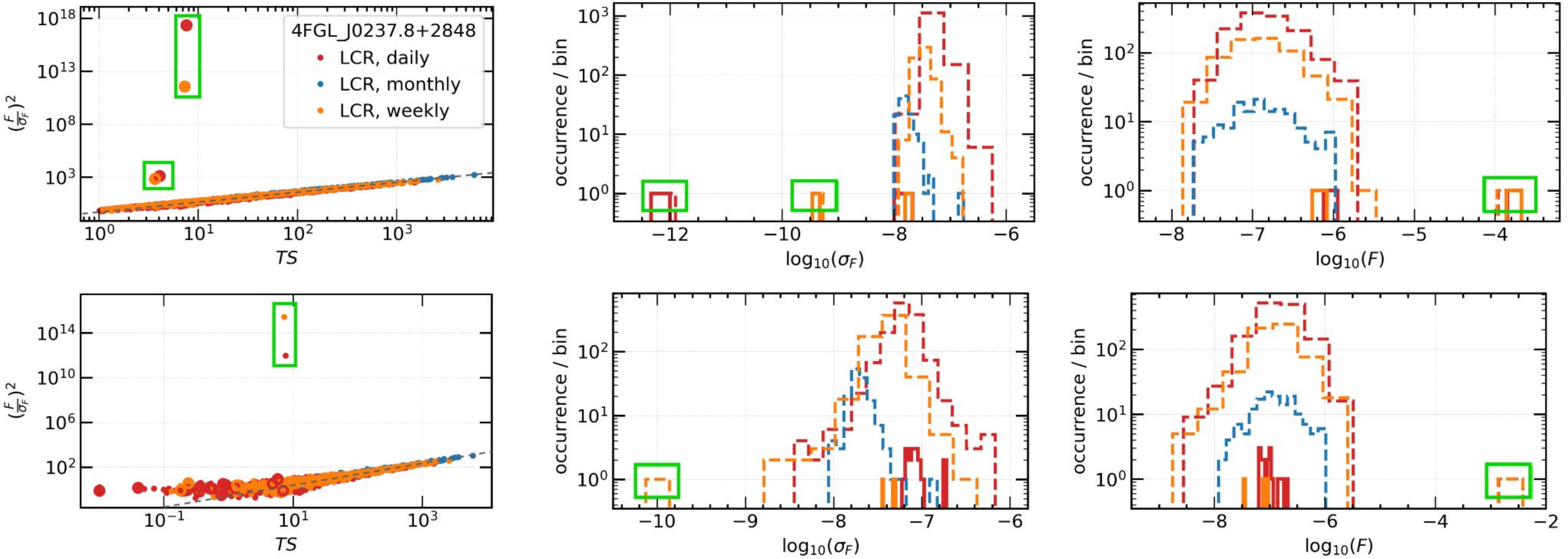

FSRQ 4C +28.07 (0.1–100 GeV): Top panels show the case for which the spectral index is fixed. The bottom panels show the case for which the spectral index is free to vary. The ratio of flux to flux uncertainty (left panels) is expected to be approximately proportional to the square root of the test statistics.

Independent exposure analysis

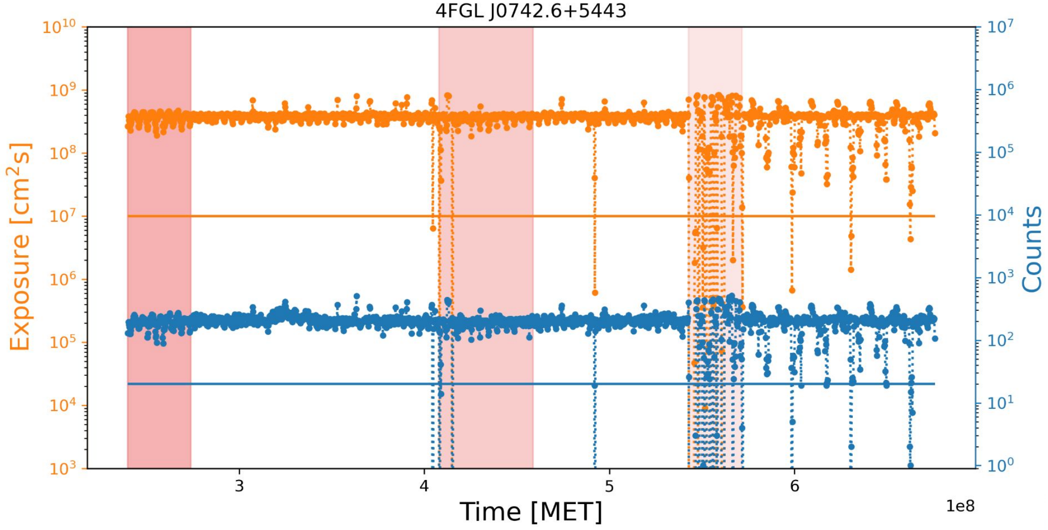

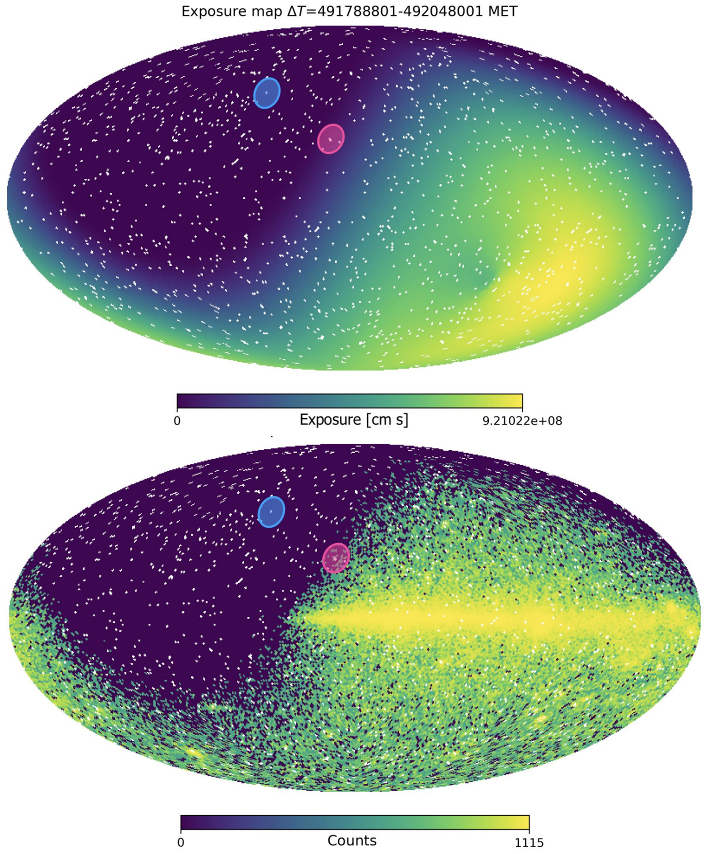

LCR pipeline does not save exposure files: Independent analysis to obtain all-sky exposure maps for each time range & estimate exposure for each LCR source ROI (i.e. 2.6K instead of 4M analyses). FSRQ GB6 J0742+5444 In the example above.

Scientific impact: Analysis methods

- Modeling weekly-timescale gamma-ray variability in blazars with self-supervised deep learning (Brill 2023, arXiv:2302.07700).
  - Model predicts the flux probability distribution at each time step.
  - Extract info on weekly-timescale flux distributions over time or between sources.

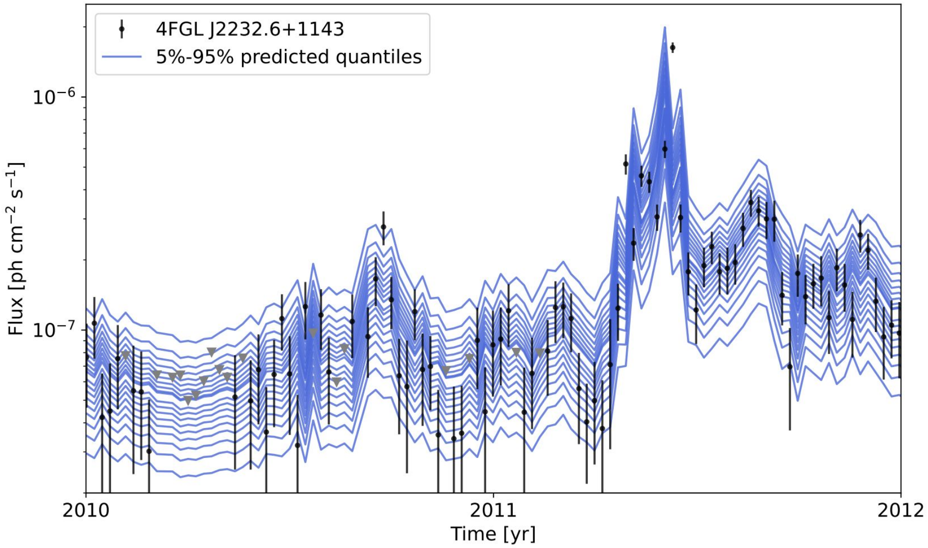

- LCR scientific impact discussions: arXiv.2210.12875, arXiv: 2308.12709.

Scientific impact: Search for periodicity

- Quasi periodic oscillations (QPO) in AGN might indicate the presence of supermassive black hole binary systems or a precessing jet.
- Possible QPOs in optical data. Possible jet precession in radio observations. No conclusive QPO detection in γ-rays.
- Analysis must include trial factors (look-elsewhere effect).
- QPO studies with LCR data:
  - MWL periodicity search in a sample of γ-ray bright blazars (MNRAS 2023, 518, 57880).
  - Detection of possible transient QPOs in the γ-ray LC of PKS 0244-470 & 4C+38.41 (ApJ 2023, 950, 173).
  - A 31.3 day Transient QPO in γ-ray emission from blazar S5 0716+714 (ApJ 2022, 938, 8).

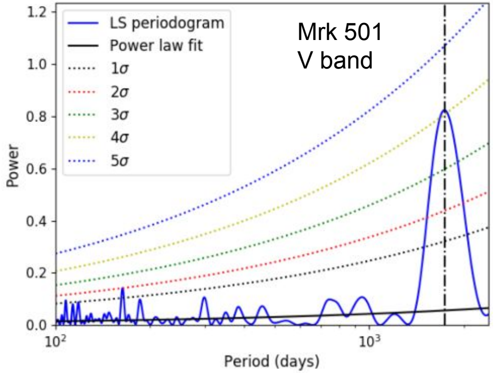

MNRAS 2023, 518, 57880

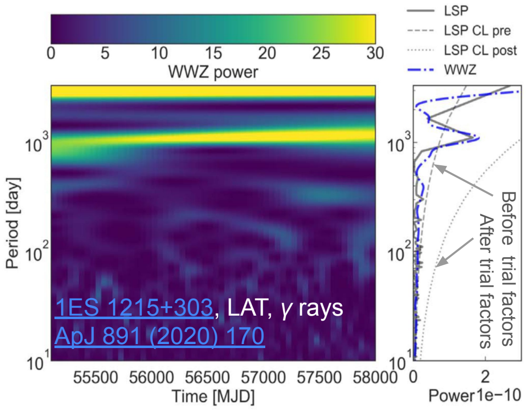

Scientific impact: Flares & correlations

- Optical/γ-ray blazar flare correlations: understanding the high-energy emission process using ASAS-SN and *Fermi* LCs [MNRAS 2023, 519, 6349](https://example.com).
- Proton synchrotron, an explanation for possible extended VHE gamma-ray activity of TXS 0506 +056 in 2017 ([PhysRevD.106.123005](https://example.com)).
- Spectroscopic reverberation mapping of Quasar PKS 0736 + 017: broad-line region and black-hole mass ([MNRAS 2022, 516, 2671](https://example.com)).

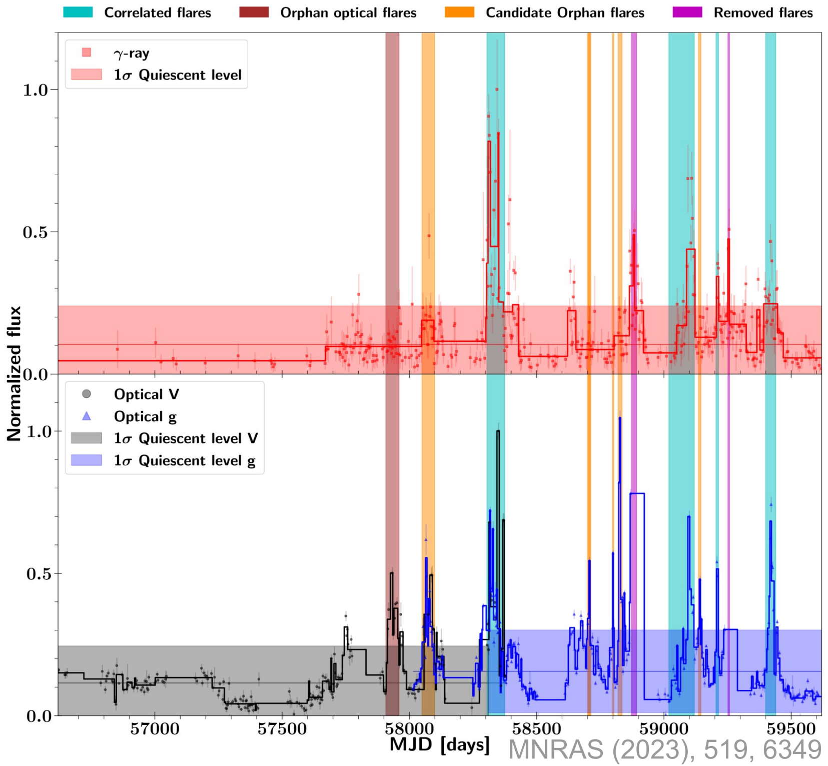

MNRAS (2023), 519, 6349

Enabling science: Community alerts

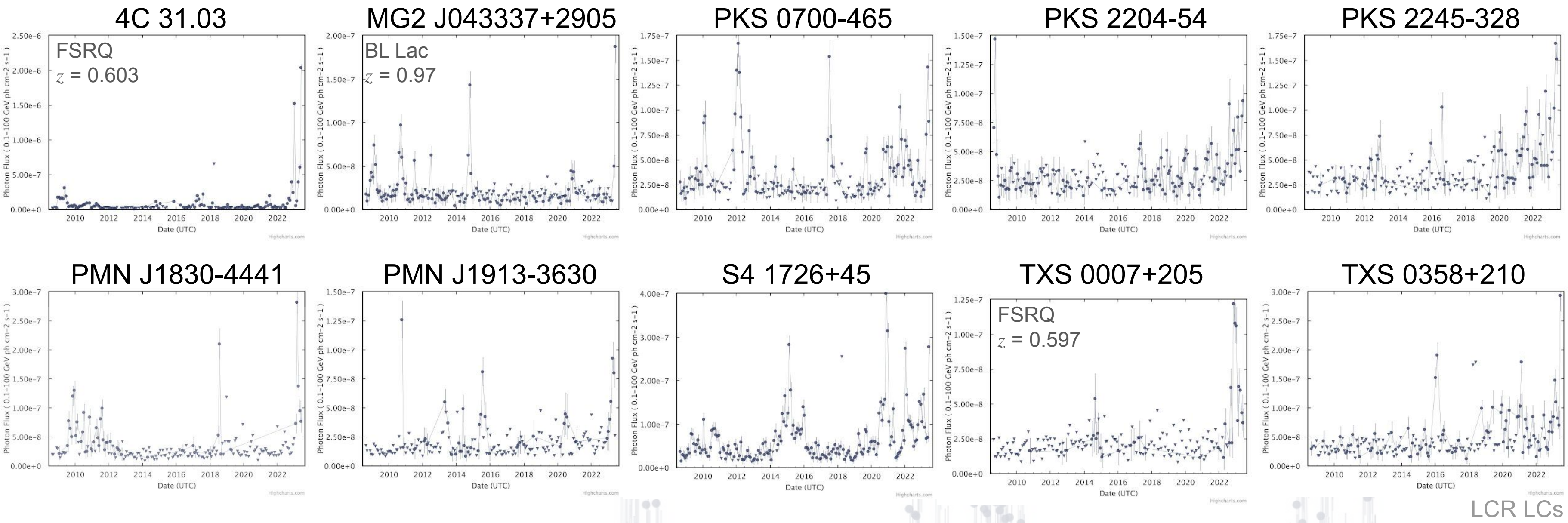

- > 52 Astronomer's Telegrams and Gamma-ray Circular Notices: https://www.glast.stanford.edu/cgi-bin/pub_rapid.
- Soon in astro-colibri.com.

Future work

- High level analyses of LCR data.
  - Flare selection to trigger alerts.
  - Variability characterization.
  - Spectral study.
- Next LCR reprocessing considered for 5FGL.

User support: fermilcr@athena.gsfc.nasa.gov
Contribute through: GitHub Repository
Cite the LCR: ApJS (2023), 265, 31 & webpage.

Thank you!